

Comparison of Solubility and Vapor Sensing Properties of Methyl- and Thiophene-Terminated Alkanethiol-Protected Gold Nanoparticle Films

HEEJOON AHN,¹ AMOL CHANDEKAR,² BONGWOO KANG,²
CHANGMO SUNG,³ AND JAMES E. WHITTEN²

¹Department of Molecular System Engineering and Graduate School of Fiber and Polymer Engineering, Hanyang University, Seongdong-gu, South Korea

²The Department of Chemistry and Center for Advanced Materials, The University of Massachusetts Lowell, Lowell, MA, USA

³School of Nanoengineering, Inje University, Gimhae, Gyeongnam, South Korea

Gold nanoparticles, protected by monolayers of two different lengths of methyl- and ω -thienyl-terminated alkanethiols, have been synthesized, and their solubility properties in various solvents have been evaluated by measuring the energy of the plasmon band using UV-Vis absorbance spectroscopy and by transmission electron microscopy. Chemical sensors have been fabricated by spin-coating films of the monolayer-protected gold particles onto interdigitated microelectrode arrays. Exposure to chloroform, toluene, and hexane vapors causes the electrical resistance of the films to increase. A sensor based on 12-(3-thienyl)dodecanethiol is shown to be dramatically more sensitive to both chloroform and toluene than one based on tridecanethiol. However, in the case of hexane, these two alkanethiol-protected gold nanoparticle sensors perform similarly. These results suggest that for very nonpolar solvents such as hexane, the functional group at the periphery of the particle is much less significant than the effect of alkanethiol chain length.

Keywords alkanethiols, gold, nanoparticles, sensors, thiophene

Introduction

We recently reported the synthesis and characterization of gold nanoparticles protected by monolayers of thiophene-terminated alkanethiols and the use of their films as organic vapor sensors (1). The mechanism of chemical sensing involves swelling of the film upon exposure to organic vapor, causing an increase in the distance between neighboring gold particles. The degree of swelling generally depends on how well the films solvate the vapor. Because electrical conductivity is due to electron tunneling and hopping between nearby gold cores, it is sensitive to interparticle distance, and exposure to organic vapor usually results in an increase in electrical resistance of the films.

Received and Accepted March 2005

Address correspondence to James E. Whitten, The Department of Chemistry and Center for Advanced Materials, The University of Massachusetts Lowell, Lowell, MA, USA 01854-5047. Tel.: (978) 934-3666; E-mail: james_whitten@uml.edu

Originally developed by Wohltjen and Snow (2), we have found these sensors to be remarkable in that they exhibit fast and reversible response. By simultaneously employing multiple films made from differently functionalized alkanethiol-protected gold nanoparticles, it should be possible to assemble a selective organic vapor sensor. While a variety of alkanethiols have been investigated (3–7), few studies have been carried out comparing the relative sensitivities of different types of alkanethiol-protected gold nanoparticle films.

Factors affecting sensor performance of organic-coated gold nanoparticle films include the dimensions of the gold cores and the chemical functionality and thickness of the molecular films comprising their coating (8). The dimensions of the gold cores are determined by the synthetic conditions during particle growth, and the organic layer thickness is determined by the length and adsorption geometry of the alkanethiol. Optimum gold nanoparticle diameters appear to be in the 1–5 nm range, and it is critical that neighboring gold particles not coalesce and fuse. In addition to imparting selectivity due to its chemical functionality, the organic layer must remain intact to prevent coalescence of the particles. It is also important that the organic layer be thick enough to solvate the vapor to be detected, but not so thick that a lack of sensitivity is realized as a result of a relatively small change in the distances between the gold particles.

In the present study, we report a comparison of the solubility properties of two different lengths each of methyl- and thiophene-terminated alkanethiol-protected gold nanoparticles and the vapor sensing properties of their films. Solubility has been evaluated by comparison of the energy of the plasmon absorption bands of the gold particles in different solvents and by transmission electron microscopy. Vapor sensors have been prepared by spin-coating films of the monolayer-protected gold nanoparticles onto interdigitated microelectrode arrays and measuring their changes in electrical resistance upon exposure to different concentrations of organic vapors.

Experimental

Materials and Syntheses

Methyl- and thiophene-terminated alkanethiol functionalized gold nanoparticles have been synthesized using the two-phase approach described by Brust (9). Reagents and solvents were purchased from Sigma-Aldrich and used as received.

12-(3-thienyl)dodecanethiol and 2-(3-thienyl)ethanethiol are not commercially available and were synthesized as previously described (10). To synthesize the nanoparticles, gold chloride (HAuCl_4) is transferred using a phase-transfer reagent into a toluene solution of the alkanethiol and subsequently reduced by adding aqueous sodium borohydride (NaBH_4). As neutral gold particles nucleate and begin to grow competitively, the alkanethiol reacts with the neutral gold surfaces to form gold-sulfur thiolate bonds. Particle growth is terminated when their surfaces are completely covered by a monolayer of the alkanethiol. The average nanoparticle size depends on the Au/thiol molar ratio.

The detailed procedure is as follows. An aqueous solution of HAuCl_4 (2.5×10^{-2} M) is stirred vigorously while adding a 7.5×10^{-2} M solution of tetraoctylammonium bromide in toluene. Stirring is continued for ca. 15 min. to ensure complete transfer of gold into the organic layer. Disappearance of the faint yellow color of the aqueous phase and appearance of a reddish-orange coloration indicate transfer of gold from the aqueous phase to the organic phase. A 10 ml solution (1.7×10^{-2} M) of the alkanethiol,

dissolved in toluene, is then added drop-wise while stirring. A 50 ml aqueous solution (0.11 M) of sodium borohydride is then added over a period of 30 min; the color of the organic phase changes immediately from reddish orange to dark violet upon addition of a few drops of the NaBH₄ solution. The mixture is allowed to stir vigorously for ca. 16 h. The organic phase is then separated from the aqueous phase and concentrated to ca. 3 ml by rotary evaporation. This concentrated solutions is then diluted to 300 ml with ethanol and stored overnight at -76°C . The solution is then filtered through a 2.5 micron polypropylene membrane filter. The portion that does not pass through the filter contains the functionalized gold nanoparticles and is washed with 10 ml of acetone and exhaustively with 1200 ml ethanol.

Characterization and Film Preparation

Characterization. UV-Visible absorbance spectroscopy has been performed using a Lambda 1806 spectrometer and an approximate concentration of 0.1 mg/ml. Transmission electron microscopy (TEM) images have been obtained using a Philips EM 400t microscope fitted with a LaB₆ filament at 120 keV. The samples for TEM are prepared by drop-casting films from 0.1 mg/ml nanoparticle solutions onto a carbon-coated copper grid.

Film Preparation. Nanoparticle films have been prepared by spin-coating from 0.1 mg/ml solutions (in chloroform) at 500 rpm onto interdigitated array (IDA) microelectrodes (Microsensor Systems, Inc. Part No. M1450110). This type of IDA microelectrode is comprised of 50 pairs of gold electrode digits (fingers) deposited on a quartz substrate with the following dimensions: 15 μm electrode width, 15 μm spacing, 4800 μm overlapping length, and 1500 \AA electrode thickness. The conductivity, σ , can be calculated by the following equation (11, 12):

$$\sigma = \frac{d \times I}{(2n - 1) \times L \times h \times V} \quad (1)$$

where d is the electrode spacing, I is current, n is the number of electrode digits, L is the overlapping length of the electrodes, h is the film thickness, and V is the bias voltage. This equation is valid for cases in which the thickness of the films does not exceed that of the gold electrodes, as in the present study. For the results reported here, a DC voltage of 2.0 V has been used. Ohmic behavior has been observed in this voltage range, and the I-V curve passes through the origin, within the noise of the experiment.

Exposing the IDA microelectrode films to organic vapors and measuring the electrical resistance changes of the films allow measurement of the vapor sensing properties of the gold nanoparticle films. This has been accomplished by installing the IDA microelectrode being investigated in a homemade chamber consisting of a small (2.50 in \times 2.25 in \times 1.38 in) airtight aluminum box fitted with electrical feedthroughs for contacting to the sample. Toluene, chloroform, and hexane vapors of varying concentration are generated by bubbling dry nitrogen gas through the solvent of interest and mixing the saturated nitrogen gas with pure dry nitrogen. These are admitted to the chamber via stainless steel tubing, with the flow rates of the saturated and pure gases measured by digital flow meters. Concentrations are calculated from the partial pressure of the saturated vapor at room temperature. All films exhibit fast response and complete reversibility. Upon exposure, 90% of the maximum response is reached within 3–4 sec. The resistance

returns to its initial value when exposure to the organic vapor is terminated by closing the bubbler. The typical overall drift in the experiment is less than 10%, even after several hours. However, we have observed changes in the electrical properties of the films due to long-term storage in air.

Results and Discussion

The solubility of monolayer-protected gold nanoparticles may be evaluated by measuring the energy of the gold plasmon absorption band. Figures 1–3 show UV-Vis spectra of ca. 0.1 mg/ml solutions of 12-(3-thienyl)dodecanethiol-, 2-(3-thienyl)ethanethiol-, tridecanethiol-, and propanethiol-protected gold nanoparticles dissolved in chloroform, toluene, and hexane, respectively. In all three solvents, the particles covered with the longer thiophene-terminated and methyl-terminated alkanethiols exhibit greater solubility, as evidenced by absorbance at shorter wavelengths, which is consistent with less agglomeration and smaller particle size. For dissolution in both chloroform and toluene, absorbance maxima for the longer chain-covered particles are ca. 515 nm. In chloroform, the 2-(3-thienyl)ethanethiol-covered particles exhibit an absorbance maximum at only slightly longer wavelength, while propanethiol-covered particles show a broad absorption band peaked near 580 nm. In the case of toluene, both of the shorter chain-covered particle solutions have absorbance maxima near 660 nm. For hexane solutions, the tridecanethiol-protected nanoparticle solution has an absorbance maximum at 480 nm, the other monolayer-protected particle solutions absorb longer wavelength light, with absorption

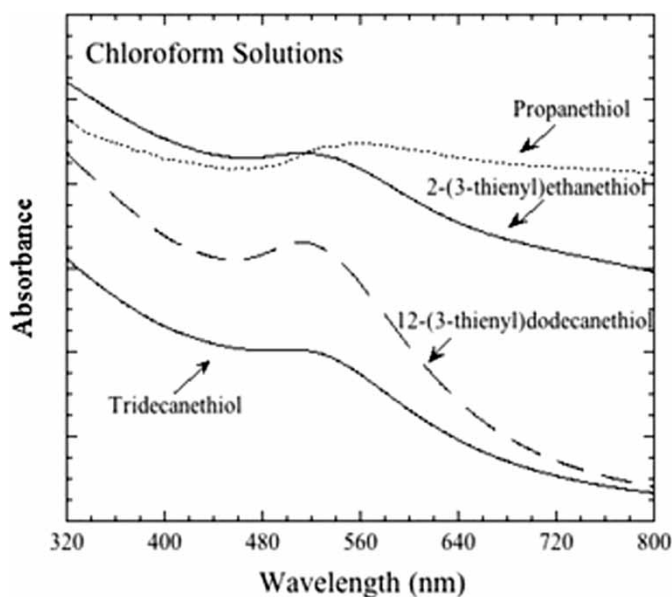


Figure 1. UV-Vis absorption spectra of solutions of gold nanoparticles protected by 12-(3-thienyl)-dodecanethiol, 2-(3-thienyl)ethanethiol, tridecanethiol, and propanethiol in chloroform. The approximate concentrations of the solutions were 0.1 mg/ml. The propanethiol spectrum has been multiplied by 3 for ease of viewing.

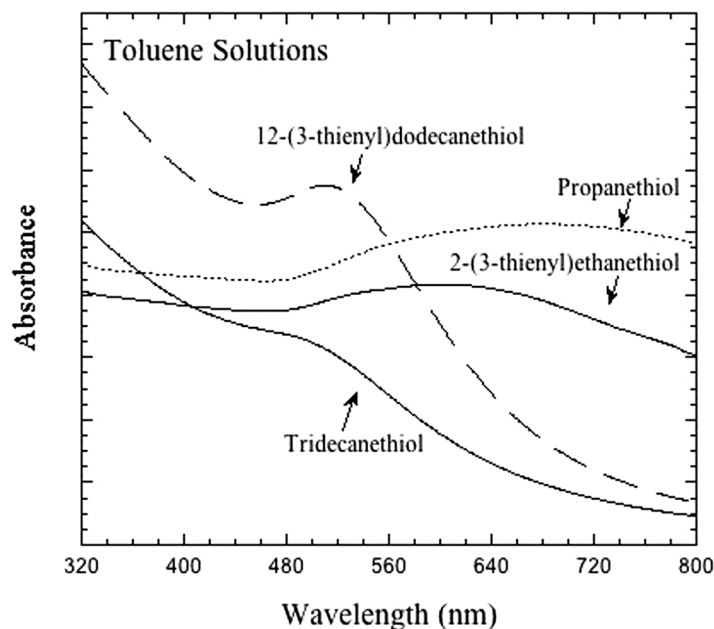


Figure 2. UV-Vis absorption spectra of solutions of gold nanoparticles protected by 12-(3-thienyl)-dodecanethiol, 2-(3-thienyl)ethanethiol, tridecanethiol, and propanethiol in toluene. The approximate concentrations of the solutions were 0.1 mg/ml. The propanethiol and 2-(3-thienyl)ethanethiol spectra have been multiplied by 2 for ease of viewing.

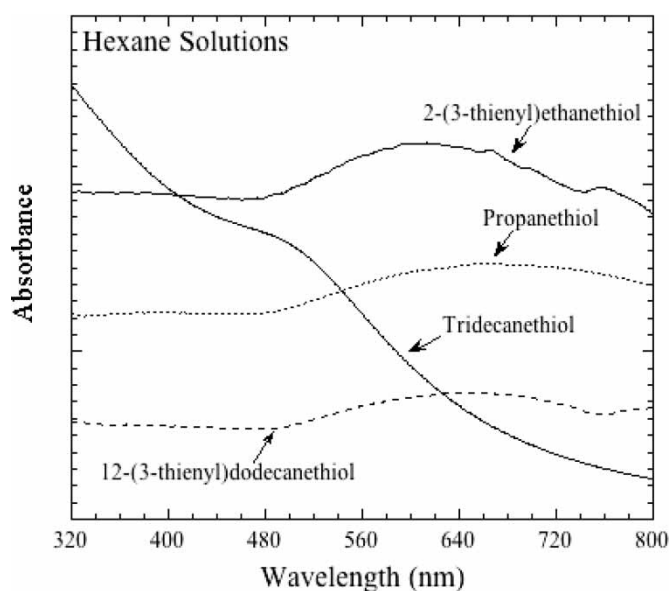


Figure 3. UV-Vis absorption spectra of solutions of gold nanoparticles protected by 12-(3-thienyl)-dodecanethiol, 2-(3-thienyl)ethanethiol, tridecanethiol, and propanethiol in hexane. The approximate concentrations of the solutions were 0.1 mg/ml. The propanethiol and 2-(3-thienyl)ethanethiol spectra have been multiplied by 2 for ease of viewing.

maxima in the range of 600–640 nm. These results indicate that all the particles, with the exception of the propanethiol-covered ones, are very soluble in chloroform. Only the longer chain-covered particles are soluble in toluene, and the UV-Vis data demonstrate that hexane solubilizes only the tridecanethiol-covered particles.

The TEM images presented in Figures 4–6 are consistent with the UV-Vis results. As shown in Figure 4, very little agglomeration is observed for the tridecanethiol-covered gold nanoparticles in both chloroform and hexane. This is in contrast to the propanethiol-covered particles, shown in Figure 5, which are agglomerated in both of these

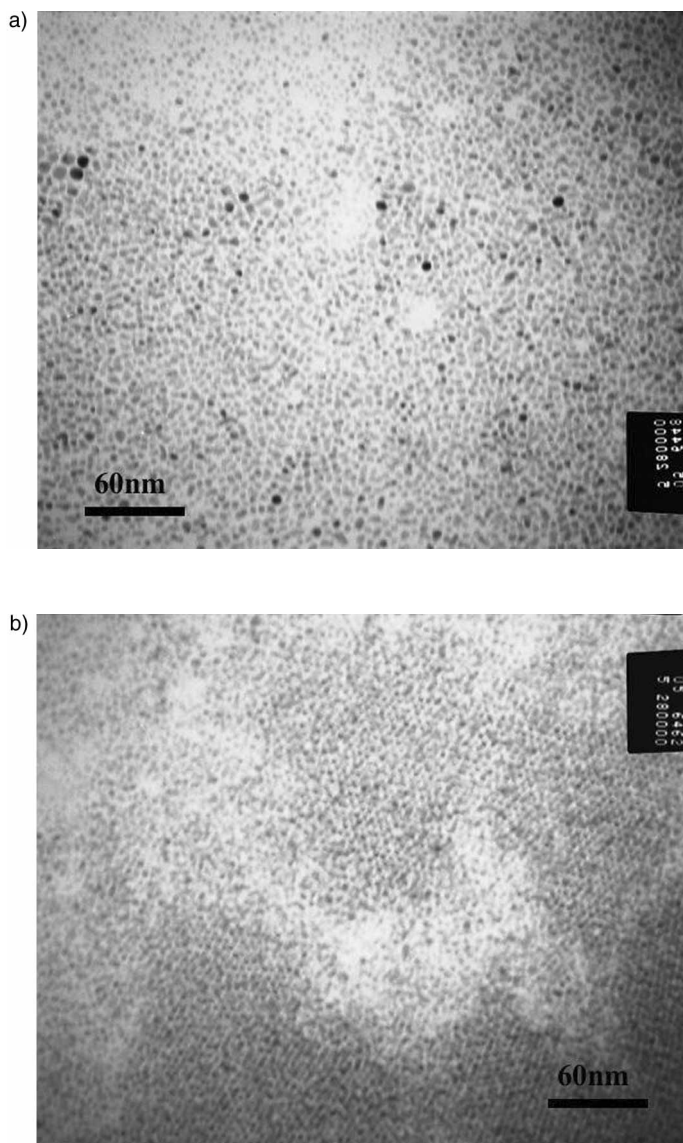


Figure 4. TEM micrographs of drop-cast films of tridecanethiol-protected gold nanoparticles using two different solvents: a) chloroform and b) hexane.

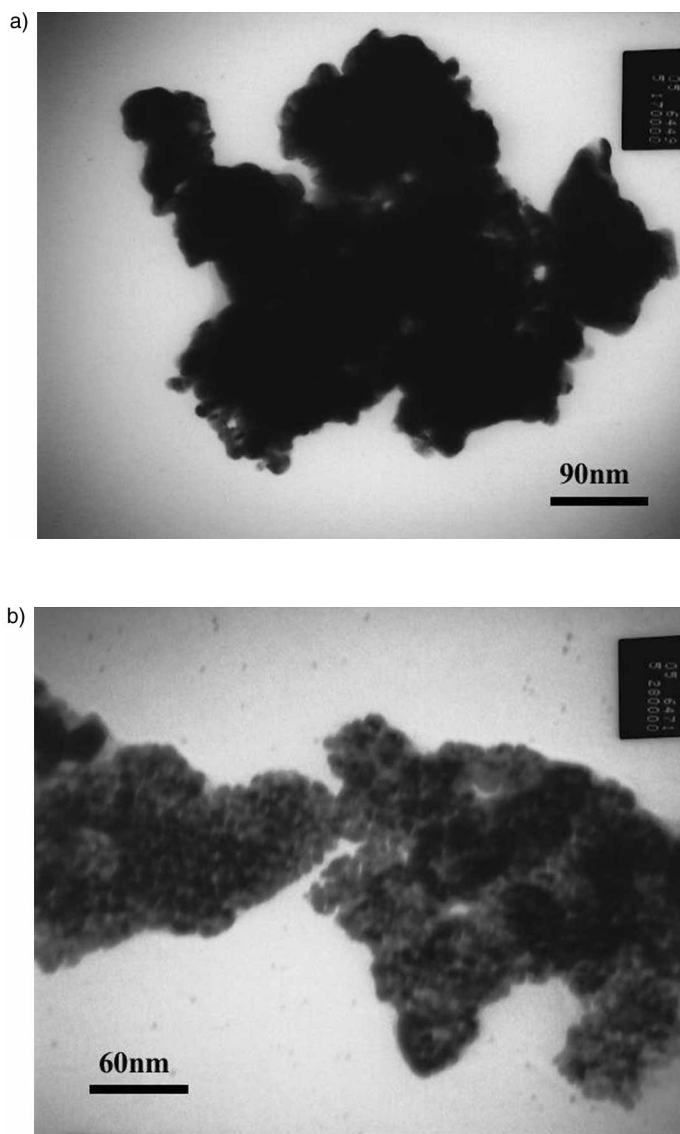


Figure 5. TEM micrographs of drop-cast films of propanethiol-protected gold nanoparticles using two different solvents: a) chloroform and b) hexane.

solvents. In the case of the 12-(3-thienyl)dodecanethiol-covered particles, whose TEM images are presented in Figure 6, the particles are agglomerated in hexane but not in chloroform. Examination of the TEM images obtained from a solvent in which the particles are soluble (e.g., chloroform) indicates that the average diameter of the metal core for all of the nanoparticles investigated in the present work is 4 nm, with an estimated error of ± 1 nm. This was confirmed by X-ray photoelectron spectroscopy analyses of nanoparticle films, as described in Reference 1. It was also confirmed, by studying the S 2p XPS peaks, that thiolate-Au bonds are present for the four monolayer-protected particle films. In the case of the thiophene-terminated particles,

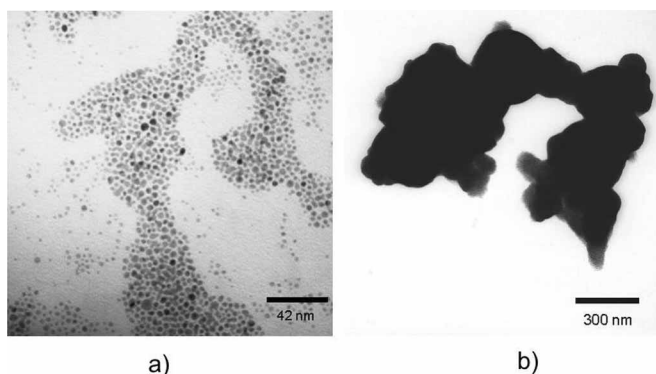


Figure 6. TEM micrographs of drop-cast films of 12-(3-thienyl)dodecanethiol-protected gold nanoparticles using two different solvents: a) chloroform and b) hexane.

the S 2p spectra exhibited peaks consistent with intact thiophene and thiolate-Au bonds. The significance of this is that these demonstrate, as expected, that the thiophene-terminated alkanethiols do not adsorb via the thiophene rings to the gold particles. This is consistent with our previous work in which self-assembly was carried out on gold surfaces (10).

Figure 7 displays a plot of the vapor-induced change in resistance divided by the initial resistance vs. chloroform vapor concentration for the four nanoparticle films. The order of sensitivities to chloroform are 12-(3-thienyl)dodecanethiol > tridecanethiol > propanethiol \geq 2-(3-thienyl)ethanethiol. Figure 8 shows data for toluene vapor.

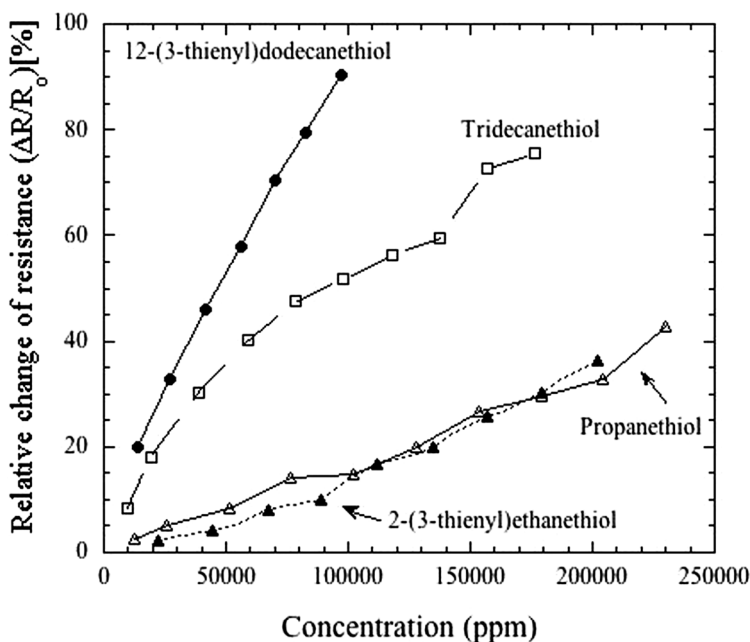


Figure 7. Response of the nanoparticle gold films to chloroform vapor. The lines through the data are included to guide the eye.

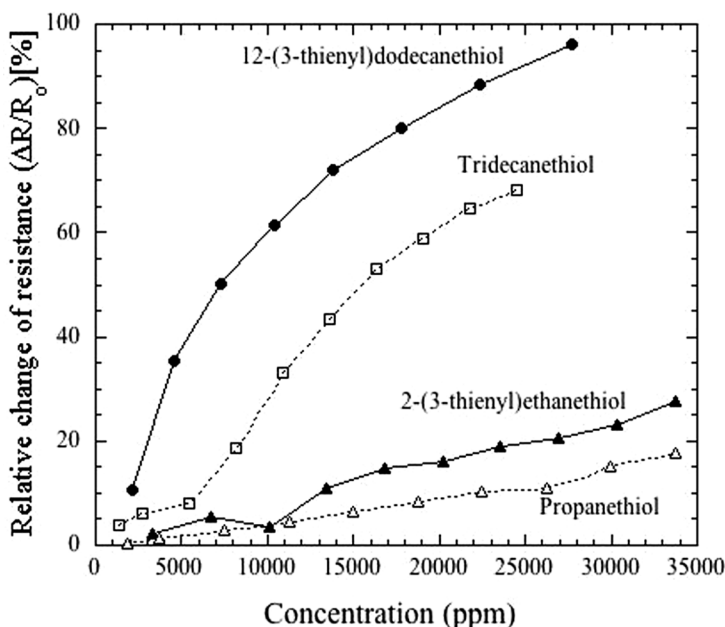


Figure 8. Response of the nanoparticle gold films to toluene vapor. The lines through the data are included to guide the eye.

In the case of toluene, the same relative orders are observed, except that the 2-(3-thienyl)ethanethiol-covered films are significantly more sensitive than the propanethiol-covered nanoparticle films. The aforementioned results are in contrast to the hexane results, shown in Figure 9. In the case of hexane vapor, nanoparticles coated with 12-(3-thienyl)dodecanethiol and tridecanethiol show very similar sensitivities, which are ca. four times greater than the sensitivities for hexane exhibited by both of the shorter-chain covered particle sensors.

In general, these results indicate that the trends in sensitivity of the films to organic vapors agree with the solubilities of the particles in the corresponding solvent. The exception to this is the similarity in the responses of the films made from 12-(3-thienyl)dodecanethiol- and tridecanethiol-covered particles to hexane vapor. The results of Figure 9 suggest that for nonpolar solvents such as hexane, the nature of the functional group (e.g., methyl versus thiophene) does not significantly affect the sensitivity of the film to that vapor; much more important seems to be the length of the alkyl chain.

Examination of Figures 7–9 and comparison of the response of a sensor to a particular concentration (e.g. 20,000 ppm) show that the 12-(3-thienyl)dodecanethiol-coated gold nanoparticle film exhibits the following order of sensitivity: toluene > chloroform > hexane. For the tridecanethiol-protected particles, the order is: toluene > chloroform = hexane. In the case of 2-(3-thienyl)ethanethiol, the order is toluene > chloroform > hexane, for propanethiol, it is toluene > chloroform = hexane.

Conclusions

Two different lengths of thiophene- and methyl-terminated alkanethiol-protected gold nanoparticles have been examined with respect to their solubility properties and vapor

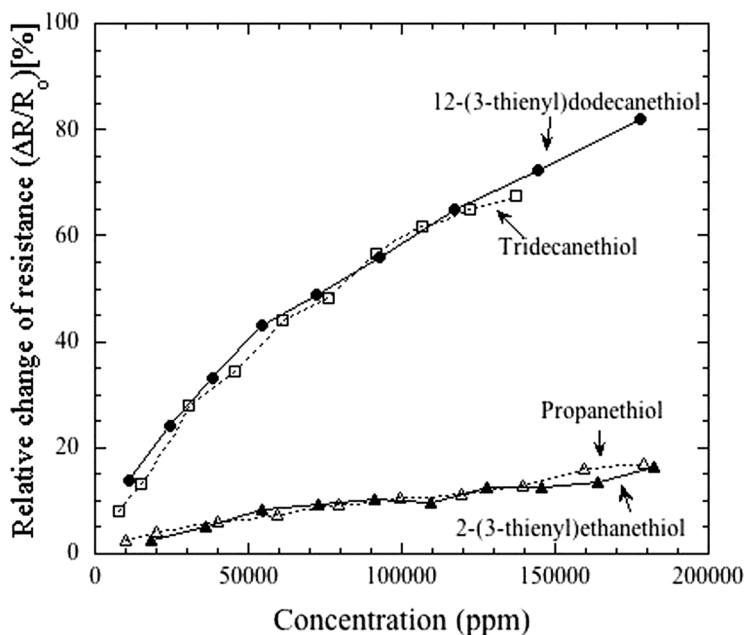


Figure 9. Response of the nanoparticle gold films to hexane vapor. The lines through the data are included to guide the eye.

sensing responses of their films. As expected, the longer chains (12 vs. 2 methylene units) result in greater solubility in chloroform and toluene. In the case of hexane, the 12-(3-thienyl)dodecanethiol-protected particles exhibit agglomeration, as evidenced by the energy of the gold plasmon band and TEM. Considering this, it is somewhat surprising that the 12-(3-thienyl)dodecanethiol film performs as well as it does with respect to vapor sensing of hexane; it performs similarly to tridecanethiol-covered gold nanoparticle films. This suggests that for nonpolar solvents, solubility effects and the nature of the functional group may be less important than other factors, such as chain length.

A benefit of the present type of sensor is its reversibility. The fabrication of a selective sensing device could, in principle, be achieved if two or more types of monolayer-protected gold nanoparticle films were used and simultaneously monitored. While differences are observed between thiophene- and methyl-terminated alkanethiol-protected gold nanoparticles in terms of the magnitude of resistance change, the present study demonstrates that both respond essentially in the same order: toluene > chloroform \geq hexane. This indicates that a more polar functional group than thiophene might be a better choice to complement a methyl-terminated alkanethiol-protected gold nanoparticle film in the construction of a selective sensor device.

Acknowledgments

This work is based on research partially supported by the National Science Foundation, under grant DMR-008960. H. Ahn acknowledges support from a Tripathy Memorial Graduate Fellowship.

References

1. Ahn, H., Chandekar, A., Kang, B., Sung, C., and Whitten, J.E. (2004) Electrical Conductivity and Vapor Sensing Properties of ω -(3-Thienyl)alkanethiol-Protected Gold Nanoparticle Films. *Chem. Mater.*, 16: 3274–3278.
2. Wohltjen, H. and Snow, A.W. (1998) Colloidal Metal-Insulator-Metal Ensemble Chemiresistor Sensor. *Anal. Chem.*, 70: 2856–2859.
3. Grate, J.W., Nelson, D.A., and Skaggs, R. (2003) Sorptive Behavior of Monolayer-Protected Gold Nanoparticle Films: Implications for Chemical Vapor Sensing. *Anal. Chem.*, 75: 1868–1879.
4. Han, L., Daniel, D.R., Maye, M.M., and Zhong, C.-J. (2001) Core-Shell Nanostructured Nanoparticle Films as Chemically Sensitive Interfaces. *Anal. Chem.*, 73: 4441–4449.
5. Zamborini, F.P., Leopold, M.C., Hicks, J.F., Kulesza, P.J., Malik, M.A., and Murray, R.W. (2002) Electron Hopping Conductivity and Vapor Sensing Properties of Flexible Network Polymer Films of Metal Nanoparticles. *J. Am. Chem. Soc.*, 124: 8958–8964.
6. Evans, S.D., Johnson, S.R., Cheng, Y.L., and Shen, T. (2000) Vapor Sensing using Hybrid Organic-Inorganic Nanostructured Materials. *J. Mater. Chem.*, 10: 183–188.
7. Briglin, S.M., Gao, T., and Lewis, N.S. (2004) Detection of Organic Mercaptan Vapors Using Thin Films of Alkylamine-Passivated Gold Nanocrystals. *Langmuir*, 20: 299–305.
8. Snow, A.W., Wohltjen, H., and Jarvis, N.L. (2002) MIME Chemical Vapor Microsensors. In *2002 NRL Review*; Bultman, J.D., ed.; Naval Research Laboratory: Washington, D.C., 45–55. This is also available at <http://www.nrl.navy.mil/content.php?P=02REVIEW45>.
9. Brust, M., Walker, M., Bethell, D., Schiffrin, D.J., and Whyman, R. (1994) Synthesis of Thiol-Derivatized Gold Nanoparticles in a Two-Phase Liquid-Liquid System. *J. Chem. Soc., Chem. Commun.*, 7: 801–802.
10. Ahn, H., Kim, M., Sandman, D.J., and Whitten, J.E. (2003) Self-Assembled Monolayers of ω -(3-Thienyl)alkanethiol on Gold. *Langmuir*, 19: 5303–5310.
11. Snow, A.W. and Wohltjen, H. (1998) Size-Induced Metal-to-Semiconductor Transition in a Stabilized Gold Cluster Ensemble. *Chem. Mater.*, 10: 547–549.
12. Snow, A.W., Barger, W.R., Klusty, M., Wohltjen, H., and Jarvis, N.L. (1986) Simultaneous Electrical Conductivity and Piezoelectric Mass Measurements on Iodine-Doped Phthalocyanine Langmuir-Blodgett Films. *Langmuir*, 2: 513–519.